

# Human immunodeficiency virus-negative multicentric Castleman's disease coexistent with Kaposi's sarcoma on $^{18}\text{F}$ -FDG PET/CT: A case report

JAE PIL HWANG<sup>1</sup>, JIYOON KIM<sup>2</sup> and JUNG MI PARK<sup>1</sup>

Departments of <sup>1</sup>Nuclear Medicine and <sup>2</sup>Pathology, Soonchunhyang University Bucheon Hospital, Bucheon, Gyeonggi 420-767, Republic of Korea

Received October 19, 2018; Accepted December 7, 2018

DOI: 10.3892/mco.2018.1789

**Abstract.** Multicentric Castleman's disease and Kaposi's sarcoma are more frequently observed in human immunodeficiency virus (HIV)-infected patients; however, 40-50% of the cases are HIV-negative. The present study reports the case of a 61-year-old man who presented with palpable masses in the axillary and right inguinal areas. The blood test results revealed increased serum erythrocyte sedimentation rate and C-reactive protein level, with negative serological markers, including for HIV. The patient was investigated using contrast-enhanced computed tomography (CT) and fluorine- $^{18}$ fluorodeoxyglucose positron emission tomography ( $^{18}\text{F}$ -FDG PET)/CT; the images revealed multiple enlarged and intensely hypermetabolic lymph nodes in the cervical, thoracic and abdominopelvic areas. Excisional biopsy and immunohistochemical analysis were performed, which confirmed the diagnosis of HIV-negative multicentric Castleman's disease coexisting with Kaposi's sarcoma. The patient received steroid therapy followed by chemotherapy. After 4 cycles of chemotherapy, the follow-up  $^{18}\text{F}$ -FDG PET/CT scan revealed nearly complete remission of the hypermetabolic malignant lesions of the neck, axilla and thoracoabdominal region.

## Introduction

Castleman's disease (CD) is a rare atypical lymphoproliferative disorder that is usually associated with constitutional symptoms, including fever, weight loss and night sweat as well as anemia, hypergammaglobulinemia and inflammatory syndrome. CD

is generally divided into the localized (unicentric) and the multicentric form. Multicentric CD (MCD) is associated with worse prognosis among all CD subtypes, and appeared to be more frequent and closely associated with the presence of Kaposi's sarcoma (KS) during the emergence of the human immunodeficiency virus (HIV) pandemic (1). HIV-negative MCD typically presents in the sixth decade of life with lymphadenopathy and multiorgan involvement, following a more aggressive natural course (2). Human herpesvirus 8 (HHV-8) infection is present in 100% of the cases of MCD in HIV-infected patients and in 40-50% of HIV-negative cases (3). Only a few cases of coexistence of MCD and KS have been reported in the literature to date. We herein present a case of HIV-negative MCD coexisting with KS involving multiple lymph nodes in a 61-year-old HIV-negative male patient. Positron emission tomography (PET)/computed tomography (CT) imaging of the torso revealed avid  $^{18}\text{F}$ -fluorodeoxyglucose ( $^{18}\text{F}$ -FDG) uptake by multiple cervical, axillary and thoracoabdominopelvic lymph nodes.

## Case report

A 61-year-old man was referred to the Soonchunhyang University Bucheon Hospital (Bucheon, Korea) in April 2017 with fever and palpable masses in the axillary and right inguinal areas, exhibiting multiple lymphadenopathies on contrast-enhanced chest and abdominopelvic CT imaging. The laboratory findings revealed an increased erythrocyte sedimentation rate (52 mm/h; normal range, 0-30 mm/h) and C-reactive protein level (1.35 mg/dl; normal range, 0-0.5 mg/dl), with decreased albumin/globulin ratio (1.0; normal range, 1.2-1.9) and hemoglobin concentration (9.8 g/dl; normal range, 13-17 g/dl). Serology was negative for hepatitis B surface antigen, hepatitis B surface antibody and HIV markers.

$^{18}\text{F}$ -FDG PET/CT (Biograph mCT 128; Siemens Healthineers, Erlangen, Germany) revealed multiple focal and enlarged hypermetabolic lymph nodes in the cervical [neck level I-V and supraclavicular fossa; maximum standardized uptake value ( $\text{SUV}_{\text{max}}$ ) 4.8-6.1], thoracic (axillary and paravertebral region;  $\text{SUV}_{\text{max}}$  6.3-9.6) and abdominopelvic (aortocaval, left para-aortic, perisplenic, common iliac, external and internal iliac and inguinal regions;  $\text{SUV}_{\text{max}}$  6.7-9.4), as well as diffuse

---

*Correspondence to:* Dr Jung Mi Park, Department of Nuclear Medicine, Soonchunhyang University Bucheon Hospital, 170 Jomaru-ro, Wonmi-gu, Bucheon, Gyeonggi 420-767, Republic of Korea

E-mail: jmiipark@schmc.ac.kr

**Key words:** Castleman's disease, Kaposi sarcoma, human immunodeficiency virus, fluorodeoxyglucose, positron emission tomography/computed tomography

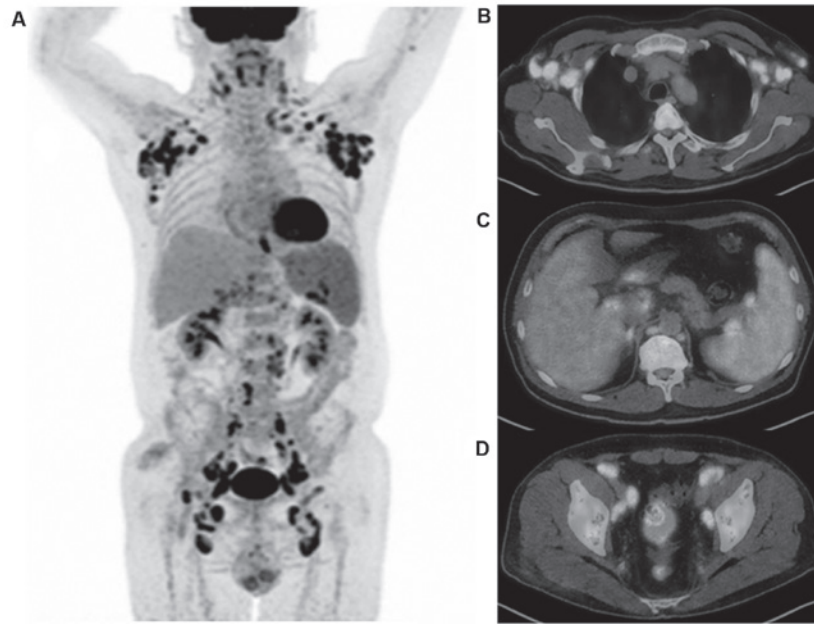


Figure 1. A  $^{18}\text{F}$ -FDG PET/CT scan was performed for evaluation of multiple lymphadenopathies. (A) MIP and (B-D) axial fusion images showing multiple hypermetabolic lymphadenopathies in the cervical (neck level I-V and supraclavicular fossa;  $\text{SUV}_{\text{max}}$  4.8-6.1), thoracic (axillary and paravertebral region;  $\text{SUV}_{\text{max}}$  6.3-9.6) and abdominopelvic (aortocaval, left para-aortic, perisplenic, common iliac, external and internal iliac and inguinal regions;  $\text{SUV}_{\text{max}}$  6.7-9.4) areas and diffuse hypermetabolic splenomegaly. FDG, fluorodeoxyglucose; PET, positron emission tomography; CT, computed tomography;  $\text{SUV}_{\text{max}}$ , maximum standardized uptake value; MIP, maximum intensity projection.

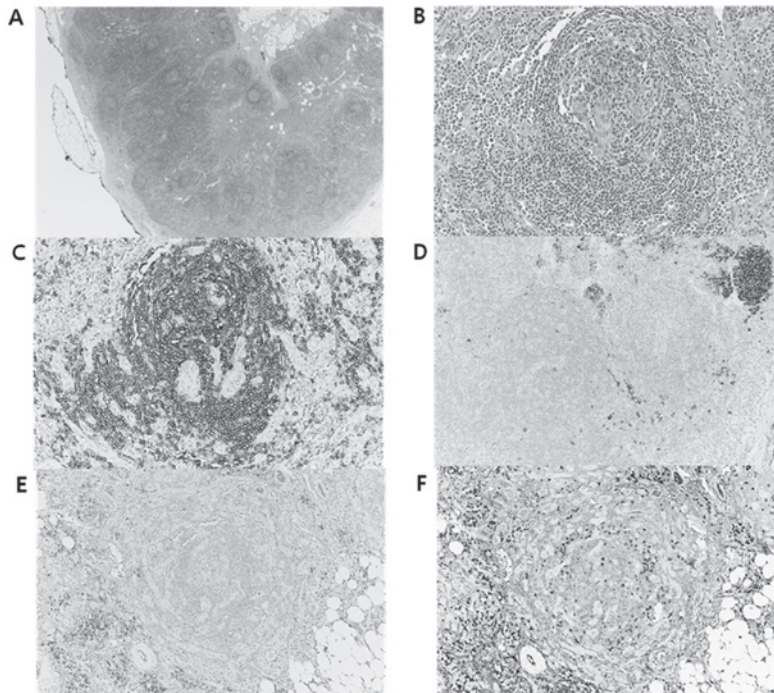


Figure 2. (A) The affected lymph nodes exhibited prominent follicles and paracortical expansion due to plasma cell infiltration on low-power magnification (x2.5). (B) The follicles had atrophic germinal centers with penetrating capillaries and concentric layers of mantle cells (onion skin sign; magnification, x200), which are diagnostic characteristics of Castleman's disease. (C) Focal vascular proliferation is observed in the same lymph node (magnification, x40). (D) Area composed of slit-like vascular spaces filled with erythrocytes (magnification, x200). (E and F) The bland looking lining cells of the vascular structures were diffusely positive for CD34 and HHV-8. (magnification, x200). HHV, human herpesvirus.

hypermetabolic splenomegaly. The  $\text{SUV}_{\text{max}}$  of the most metabolically active lesion was 9.6 (Fig. 1).

An excisional biopsy of the right inguinal and right neck lymph nodes was performed, as lymphoma was suspected on the basis of lymph node enlargement with intense FDG

uptake of the pathological lymph nodes, diffuse hypermetabolic splenomegaly, and origin from the lymphatic chains. The lymph nodes exhibited prominent follicles and paracortical expansion due to plasma cell infiltration on low-power magnification (Fig. 2A). The follicles had atrophic germinal

centers with penetrating capillaries and concentric layering of mantle cells (onion skin sign, Fig. 2B), which are diagnostic characteristics of CD. Furthermore, focal vascular proliferation was observed in the same lymph node (Fig. 2C). This area was composed of slit-like vascular spaces filled with erythrocytes (Fig. 2D). The bland-looking lining cells of the vascular structures were diffusely positive for CD34 (Fig. 2E) and HHV-8 (Fig. 2F). These immunohistochemical results supported the diagnosis of KS arising in CD. The patient was treated with oral steroid therapy for 14 days (60 mg prednisolone daily) followed by chemotherapy (730 mg rituximab and 40 mg liposomal doxorubicin intravenously, every 3 weeks for a total of 6 cycles). After 4 cycles of chemotherapy, a follow-up  $^{18}\text{F}$ -FDG PET/CT was undertaken for treatment response assessment, and it revealed a nearly complete remission of the hypermetabolic malignant lesions of the neck, axilla and thoraco-abdominal region.

## Discussion

CD, also referred to as angiofollicular lymph node hyperplasia, was first described in 1954 by Castleman and Towne (4), and is a lymphoproliferative disorder with an increased prevalence among patients with HIV infection; in that setting, it has been associated with HHV-8 and KS. CD is generally divided into the localized (unicentric) and the multicentric forms. A third subtype of CD, known as plasmablastic MCD, has also been identified, and is associated with polyneuropathy, organomegaly, endocrinopathy, monoclonal gammopathy and skin changes (5). MCD in the HIV-negative population typically presents in the sixth decade of life with lymphadenopathy and multiorgan involvement, following a more aggressive natural course (6). Approximately 13% of patients with MCD have HHV-8 infection, also referred to as KS-associated herpesvirus (KSHV). It is currently known that HHV-8 is present in 100% of the cases of MCD in patients infected with the HIV and in 40-50% of HIV-negative cases (3). Patients commonly exhibit other KSHV-associated tumors, including KS and primary effusion lymphoma, and are at high risk of developing large-cell lymphoma (4). A few cases of coexistence of MCD and KS, with or without using  $^{18}\text{F}$ -FDG PET/CT, have been reported in the literature to date. Dossier *et al* (1) and Yaghoobi *et al* (6) reported HIV-negative coexistence of MCD and KS, but those studies did not use  $^{18}\text{F}$ -FDG PET/CT. Polizzotto *et al* (7) reported 27 patients with coexistence of MCD and KS using  $^{18}\text{F}$ -FDG PET/CT, but all the included patients were HIV-positive. To the best of our knowledge, this is the first case to report HIV-negative, HHV-8-positive coexistence of MCD and KS using  $^{18}\text{F}$ -FDG PET/CT.  $^{18}\text{F}$ -FDG PET/CT is useful for evaluating the malignant potential of multiple lymphadenopathies and for the detection of distant metastasis in order to optimize treatment (8). Therefore, albeit rare, the coexistence of MCD and KS should be considered in the differential diagnosis of multiple lymphadenopathies detected by  $^{18}\text{F}$ -FDG PET/CT.

## Acknowledgements

Not applicable.

## Funding

No funding was received.

## Availability of data and materials

All data generated or analyzed during the present study are included in this published article.

## Authors' contributions

JPH and JMP conceived and designed the study. JPH and JK analyzed the data and wrote the paper. JPH and JMP reviewed and edited the manuscript. All authors have read and approved the final version of this manuscript.

## Ethics approval and consent to participate

Not applicable.

## Patient consent for publication

Patient consent was obtained for the publication of the case details and associated images.

## Competing interests

The authors declare that they have no competing interests.

## References

- Dossier A, Meignin V, Fieschi C, Boutboul D, Oksenhendler E and Galicier L: Human herpesvirus 8-related Castleman disease in the absence of HIV infection. *Clin Infect Dis* 56: 833-842, 2013.
- Mylona EE, Baraboutis IG, Lekakis LJ, Georgiou O, Papastamopoulos V and Skoutelis A: Multicentric Castleman's disease in HIV infection: A systematic review of the literature. *AIDS Rev* 10: 25-35, 2008.
- Pinto LW and Nunes EP: Simultaneous lymph node involvement by Castleman disease and Kaposi sarcoma. *Rev Bras Hematol Hemoter* 33: 73-76, 2011.
- Castleman B and Towne VW: Case records of the Massachusetts General Hospital: Case No. 40231. *N Engl J Med* 250: 1001-1005, 1954.
- Reddy D and Mitsuyasu R: HIV-associated multicentric Castleman disease. *Curr Opin Oncol* 23: 475-481, 2011.
- Yaghoobi R, Pazyar N and Tavakoli S: Co-existence of multicentric Castleman's disease and Kaposi's sarcoma. *Indian J Dermatol* 60: 323, 2015.
- Polizzotto MN, Millo C, Uldrick TS, Aleman K, Whatley M, Wyvill KM, O'Mahony D, Marshall V, Whitby D, Maass-Moreno R, *et al*:  $^{18}\text{F}$ -fluorodeoxyglucose positron emission tomography in Kaposi sarcoma herpesvirus-associated multicentric Castleman disease: Correlation with activity, severity, inflammatory and virologic parameters. *J Infect Dis* 212: 1250-1260, 2015.
- Barker R, Kazmi F, Stebbing J, Ngan S, Chinn R, Nelson M, O'Doherty M and Bower M: FDG-PET/CT imaging in the management of HIV-associated multicentric Castleman's disease. *Eur J Nucl Med Mol Imaging* 36: 648-652, 2009.